Journal of Applied Electrochemistry **34**: 1039–1044, 2004.

Improved lead–acid cells employing tin oxide coated Dynel fibres with positive active-material

B. HARIPRAKASH[1], A.U. MANE[2], S.K. MARTHA[1], S.A. GAFFOOR[3], S.A. SHIVASHANKAR[2] and A.K. SHUKLA[1,4,*]

[1]*Solid State and Structural Chemistry Unit, Indian Institute of Science, Bangalore-560 012, India*
[2]*Materials Research Centre, Indian Institute of Science, Bangalore-560 012, India*
[3]*NED Energy Ltd., 6-3-1109/1 Navbharat Chambers, Raj Bhavan Road, Hyderabad-500 082, India*
[4]*Central Electrochemical Research Institute, Karaikudi, 623 006, India*
*(*author for correspondence, fax: +91 80 23601310, e-mail: shukla@sscu.iisc.ernet.in)*

Received 9 March 2004; accepted in revised form 18 May 2004

Key words: coup de fouet, Dynel fibres, lead–acid cell, rapid-thermally-activated chemical reaction process

Absract

A rapid-thermally-activated chemical reaction process has been employed to coat tin oxide onto Dynel fibres. Positive-limited 2 V/1.5 Ah lead-acid cells employing tin-oxide coated Dynel fibres as additive to positive active mass have been assembled and characterized under various operational conditions. In this manner, it has been possible to improve the positive active material utilization and particularly at higher discharge rates.

1. Introduction

Inadequate positive active-mass utilization restricts the performance of lead–acid batteries, particularly at high discharge-rates, making it one of the major factors limiting their specific energy density. In a lead–acid battery, low positive active-mass utilization is due to poor acid transport from the bulk of the solution into the interior of the plate, and a continuous reduction in the conductivity of the plates due to formation of non-conductive $PbSO_4$. An approach to mitigating these problems has been to improve the positive plate porosity and/or its conductivity by incorporating additives into the positive active material [1]. Such an approach has received considerable attention in the development of high-drain, long-life lead–acid batteries [2–25].

Additives may also enhance the performance of the active material by altering its (i) porosity, (ii) conductivity, (iii) crystal morphology and geometry, and (iv) mechanical strength [2]. Among these, porosity, conductivity, crystal morphology and geometry of the active material influence the discharge capacity and active material utilization, while mechanical strength affects the cycle life. In the light of these factors, we have attempted to enhance the conductivity of positive plates with Dynel fibres by coating the latter with conducting tin oxide. It is well known that Dynel fibres act as excellent binder for the active material without compromising on the cycle-life of the plates by maintaining their mechanical integrity. A higher proportion of Dynel fibres in the active mass improves the porosity and helps tailor the desired electrode morphology.

In this communication, we report the performance of lead–acid cells utilizing positive plates prepared with an admixture of active mass and tin oxide coated Dynel fibres. A similar study has been reported by Lam et al. [13] by employing tin oxide coated glass flakes as an additive for positive active material in lead–acid batteries. We describe a novel, rapid thermally-activated chemical reaction process (RTACRP) for applying tin oxide coating onto Dynel fibres to enhance the lead–acid battery performance.

Preparing tin oxide by conventional methods requires a calcination process at temperatures ranging between 450 and 600 °C [26]. Hence, coating tin oxide onto low-melting substrates, such as Dynel fibres, without affecting their mechanical integrity by RTACRP is the novelty of this study. The process is simple, less time-consuming and cost-effective, and hence looks commercially attractive. Also, it is noteworthy that coating onto such thin fibres uniformly by other means (such as sputtering) is rather complex, time consuming and difficult. It has been possible to (i) accelerate the formation process, (ii) improve the positive active material utilization at higher discharge rates, (iii) tailor

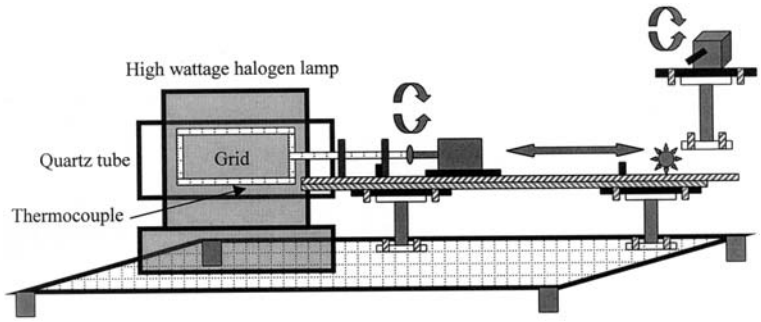

Fig. 1. Schematic diagram of RTACRP set-up.

the desired electrode morphology, and (iv) enhance the cycle-life of lead–acid cells by the aforesaid process.

2. Experimental details

A thin layer of tin oxide coating was applied onto Dynel fibres procured from M/s. Infra Chemicals, Bangalore, India, using a homemade furnace employing halogen lamps as the heating source. For this purpose, a viscous solution of stannous chloride ($SnCl_2$) was obtained by dissolving it in methanol. Dynel fibres were dipped in this solution and, subsequent to air-drying, were subjected to a coating of conducting tin oxide, employing the rapid thermally activated chemical reaction process (RTACRP). Powder X-ray diffraction pattern of the Dynel fibres before and after tin oxide coating were recorded on a Siemens D-5005 X-ray diffractometer using CuK_α-radiation at a scan rate of 2° min^{-1}. Surface morphology of the tin oxide coated Dynel fibres was studied using a Jeol JSM-5600LV scanning electron microscope.

Both positive and negative plates of the lead–acid cells were prepared using Pb–Ca–Sn–Al alloy grids to construct 2 V/1.5 Ah cells in Plexiglas containers using 1.28 specific gravity aq. H_2SO_4 as electrolyte, following an established industrial protocol. In brief, the positive plate paste was prepared by mixing PbO (85 wt %), sodium carboxy methyl cellulose (0.15 wt %), Dynel fibres (0.05 wt %), and aq. H_2SO_4 of 1.4 specific gravity (7 wt %) with de-ionised water (7.8 wt %). The negative plate paste was prepared by mixing PbO (85 wt %), lignin (0.2 wt %), barium sulphate (0.15 wt %), Dynel fibres (0.05 wt %), carbon black (0.1 wt %), and aq. H_2SO_4 of 1.4 specific gravity (7 wt %) with de-ionised water (7.5 wt %). The paste densities for positive and negative plates were 4.2 and 4.4 g cm^{-3}, respectively. In a similar way, positive plates were also prepared by mixing 2 wt % of SnO_2 coated Dynel fibres. The paste density obtained by such a mixing was 3.8 g cm^{-3}. After pasting the active materials onto the grids, the plates were subjected to hydrothermal curing.

Two different sets of three positive limited lead–acid cells were assembled with and without additive to study the effect of tin oxide coated Dynel fibres on the performance of these cells. The cells were assembled by keeping a positive electrode in between two negative electrodes. Galvanostatic charge–discharge tests at different rates between $C/5$ and $3C$, and at temperatures ranging between 40 °C and −40 °C, were conducted on such lead–acid cells employing an Autolab PGSTAT30 (EcoChemie, Utrecht, The Netherlands), with a BSTR10A current booster module and custom-built hot and cold chambers (Culture Instruments, India). Impedance measurements were also carried out on the cells using Autolab PGSTAT30. The cells were also subjected to life-cycle test at $C/5$ rate at 25 °C.

3. Results and discussion

The schematic description of RTACRP set-up employed in the present study is shown in Figure 1. During this process, the sample to be coated is heated rapidly to attain the required calcination temperature within a few seconds followed by a rapid quenching. In this manner, it has been possible to coat a surface that cannot withstand exposure to high temperature for prolonged period of time [27, 28].

The powder XRD patterns for the Dynel fibres before and after the tin oxide coating are shown in Figure 2. The powder XRD pattern of the tin oxide film on Dynel

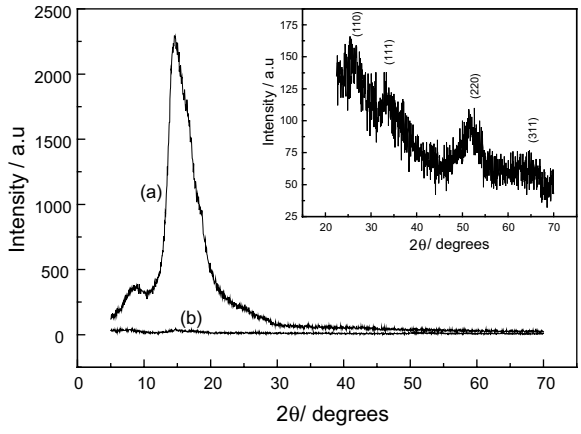

Fig. 2. Powder XRD patterns for the Dynel fibres (a) before, and (b) after tin oxide coating. Inset: exploded powder XRD pattern of tin oxide coated onto Dynel fibres.

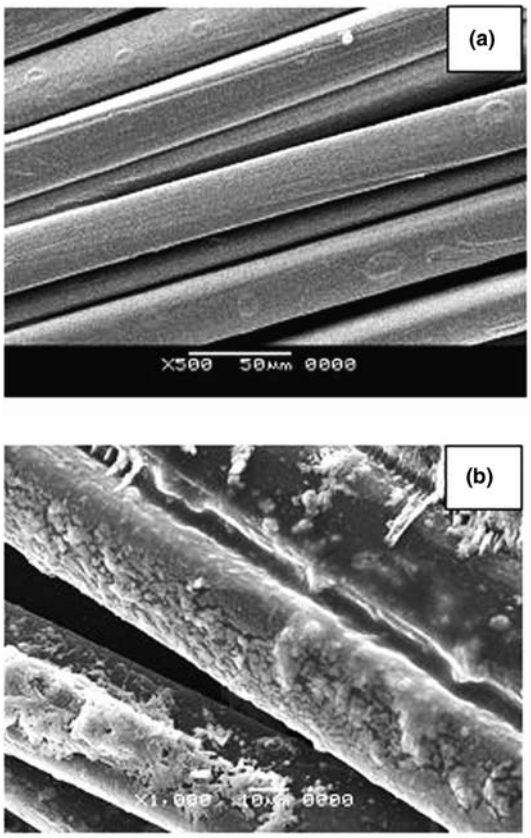

Fig. 3. Scanning electron micrographs showing the surface morphology of Dynel fibres (a) before, and (b) after tin oxide coating.

fibres prepared by rapid thermally activated chemical reaction process (RTACRP) is shown in the inset to Figure 2. The pattern agrees well with that of cubic SnO_2. Our preparative method involving rapid heating and quenching is a non-equilibrium reaction and favors the formation of tin oxide in cubic form. Indeed, tin oxide in cubic structure has been obtained by a high pressure synthesis method after laser heating and quenching [29, 30]. Surface morphology of Dynel fibres before and after tin oxide coating are shown in Figure 3 (a) and (b), respectively. The fibres are of 3 mm length with 25 μm thickness. The tin oxide coating appears to be porous and non-uniform.

2V/1.5 Ah cells were assembled and subjected to formation cycles. The additived cells were found to form within three charge–discharge cycles, while the conventional cells attained their maximum capacity in five charge–discharge cycles. During formation, the cells were charged at $C/20$ rate followed by the discharge at $C/5$ rate. A typical charge–discharge data obtained at 25 °C at $C/5$ rate for the cells with tin oxide coated and bare Dynel fibres are shown in Figure 4. It is clear that the faradaic efficiency of additived cells is superior to that of the conventional cells, and is found to be about 90%. Moreover, the additived cells deliver higher discharge capacity than do conventional cells. Furthermore, the higher plateau voltage during discharge suggests that the additived plates offer a lower internal resistance and provide a wider effective capacity window [31].

Performance characteristics of the cells at different rates ranging between $C/3$ and $2C$ are shown in Figure 5. Additived cells deliver about 60% capacity at $2C$ rate, while the conventional cells deliver only 48%. Percentage capacities obtained during discharge at different current densities at 25 °C are shown in Figure 6. It is considered that the capacity obtained is 100% at $C/5$ rate at 25 °C. There is considerable increase in the capacity of additived cells at all rates of discharge. An increase in capacity of almost 15% is seen at a discharge current density of 120 mA g^{-1}. Figure 7 shows the discharge data at $C/5$ rate at different temperatures between 40 °C and −40 °C. Additived cells perform better than conventional cells do at all temperatures. The cells deliver about 45% capacity at −40 °C.

Electrochemical impedance measurements were conducted on the positive plates using $Pb/PbSO_4$, SO_4^{2-} as the reference electrode and the charge-transfer resistance data obtained as a function of state-of-charge (SOC) are shown in Figure 8. The data depict that the charge-transfer resistance of additived positive electrodes is less

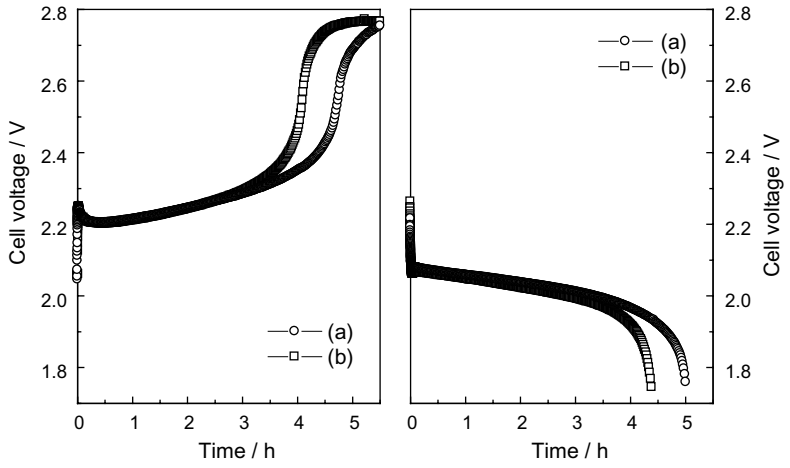

Fig. 4. Typical charge–discharge data obtained at 25 °C at $C/5$ rate for the lead–acid cells: (a) with and (b) without tin oxide additive.

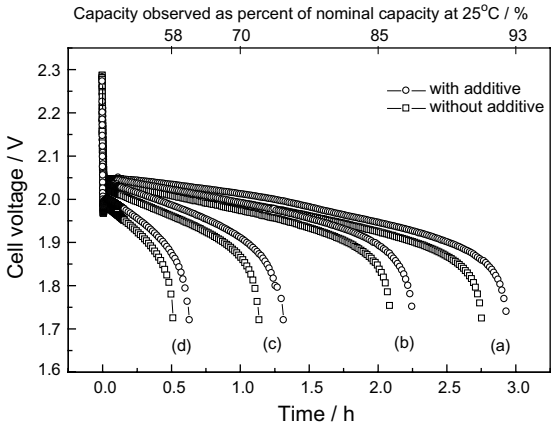

Fig. 5. Performance characteristics of the lead–acid cells with and without tin oxide additive at 25 °C at (a) $C/3$, (b) $C/2$, (c) C and, (d) $2C$ rates.

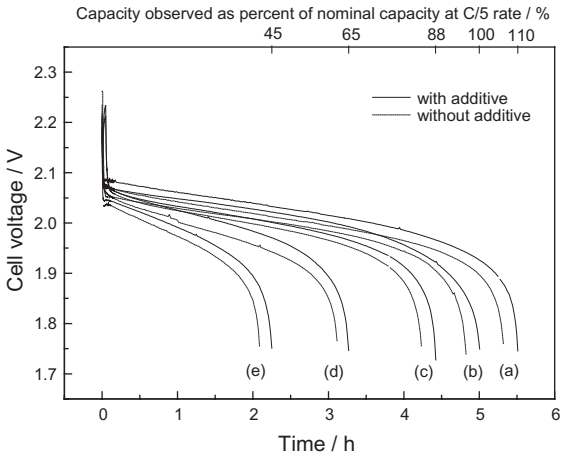

Fig. 7. Temperature-dependent performance characteristics of lead–acid cells at $C/5$ rate at (a) 40, (b) 20, (c) 0, (d) −20 and (e) −40 °C.

than the charge-transfer resistance of the conventional cells at all SOC values. Figure 9 shows the Nyquist plots obtained at SOC = 0 for positive plates with and without tin oxide additive. It is clear from Figure 9 that the ohmic resistance offered by the additived cells is less than in conventional cells. The spectra were analysed using a nonlinear least-squares fitting program [32], and it has been possible to fit the impedance plots at all SOC values to a R_Ω (R_1Q_1) (R_2Q_2) equivalent circuit, shown in the inset to Figure 9. The impedance spectrum comprising two semicircles is due to two pairs of parallel resistances and capacitances. R_Ω is the ohmic resistance, R_1 and Q_1 are the respective values for resistance and constant phase element (CPE) corresponding to the high-frequency semicircle, and R_2 and Q_2 are the respective values for resistance and CPE corresponding to the low-frequency semicircle. It is noteworthy that while R_1 is the resistance due to morphology of the porous-electrode, R_2 refers to the charge-transfer resistance for the electrode reaction. The two constant phase elements Q_1 and Q_2 refer to the capacitance due to the

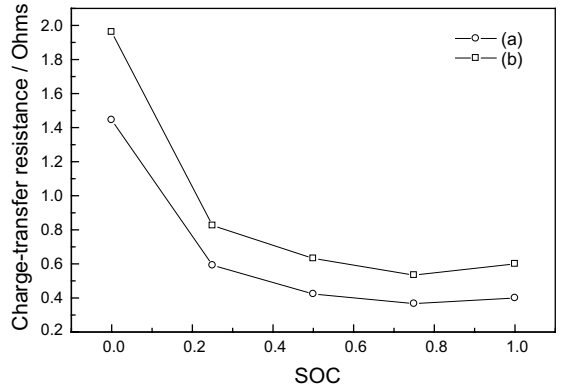

Fig. 8. Charge-transfer resistance data obtained as a function of state-of-charge for positive plates of lead–acid cells: (a) with and (b) without tin oxide additive.

porous-electrode morphology and electrode double-layer capacitance, respectively.

Electrode surface morphologies with and without tin oxide additives are shown in Figure 10(a,b) and (c,d),

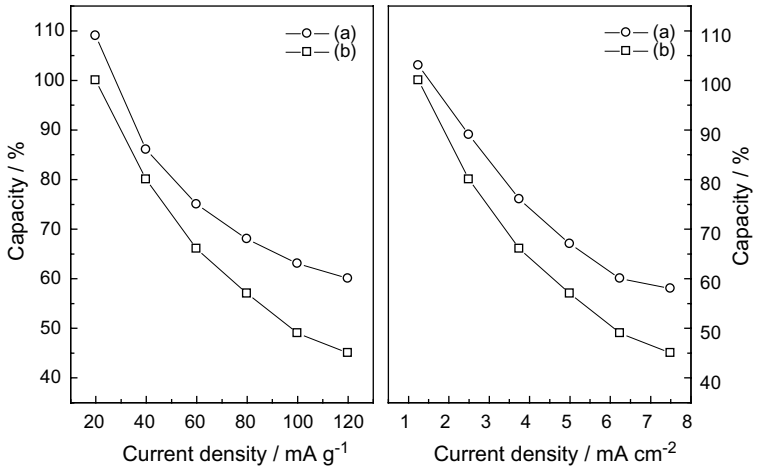

Fig. 6. Percentage capacities obtained for the lead–acid cells (a) with and (b) without tin oxide additive at different current densities at 25 °C.

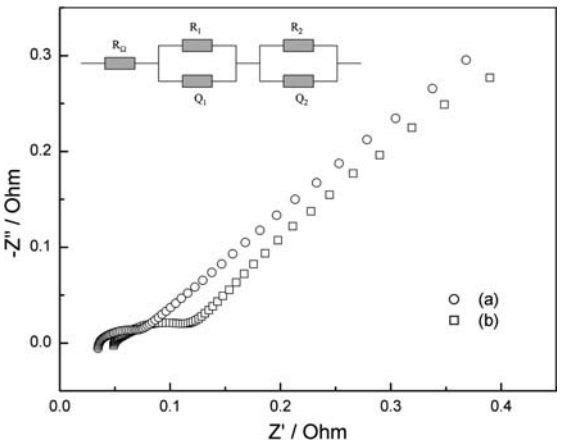

Fig. 9. Nyquist plots obtained for positive plates of lead–acid cells at SOC = 0: (a) with and (b) without tin oxide additive.

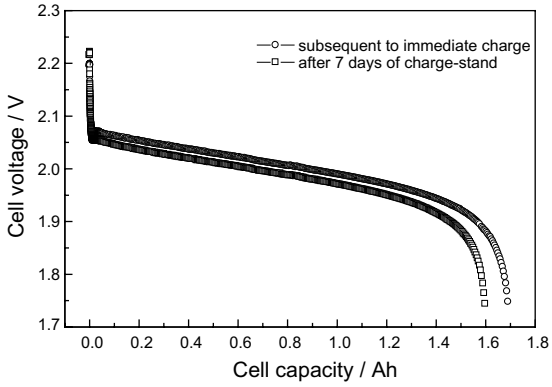

Fig. 11. Discharge data at $C/5$ rate at 25 °C for the additived lead–acid cell: (a) immediate after its charge, and (b) after charge-stand for a week.

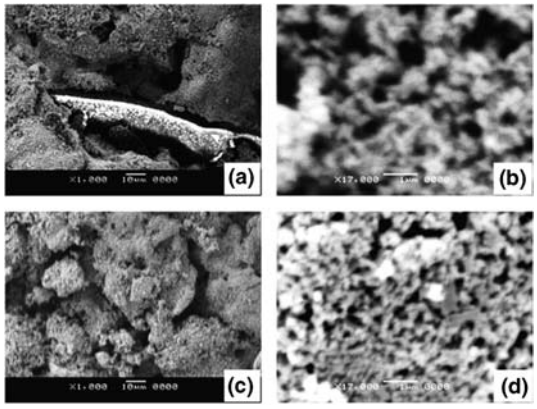

Fig. 10. Electrode surface morphologies of positive plates of lead–acid cells with (a and b) and without (c and d) tin oxide additives after 50 cycles.

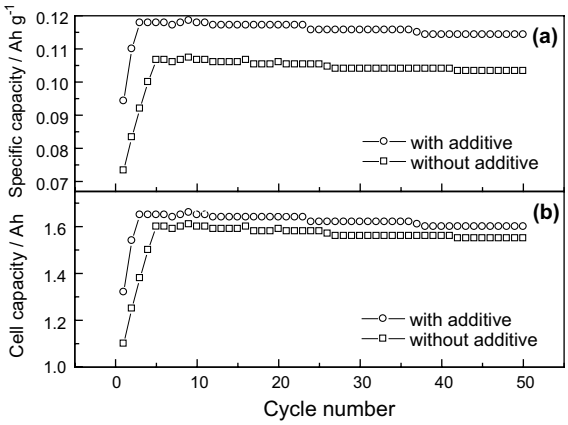

Fig. 12. Specific capacity values for the positive electrodes (a) with and without tin oxide additived Dynel fibres, and (b) capacity values for lead–acid cells employing positive electrodes with tin oxide additived Dynel fibres and conventional lead–acid cells up to 50 cycles at $C/5$ rate at 25 °C.

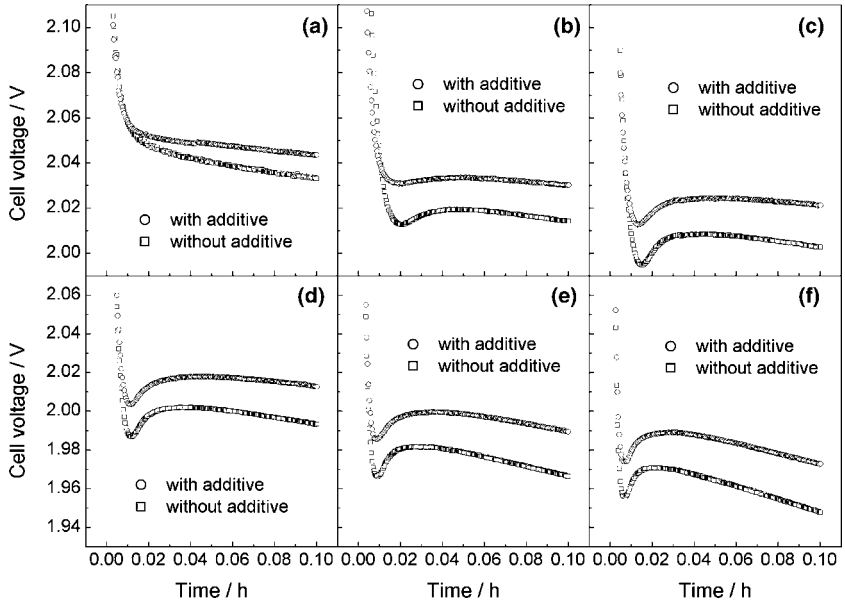

Fig. 13. Coup de fouet data for the lead–acid cells with and without tin oxide additive at various current densities: (a) 20, (b) 40, (c) 60, (d) 80, (e) 100 and (f) 120 mA g^{-1}.

respectively. It is seen from Figure 10(a) that the 5–10 μm gap between the fibre and active material provides the path for sulfuric acid to seep, which accounts for the observed higher positive active material utilization. Also, additived electrodes are more porous than those in the conventional cells, as seen from Figure 10(b).

The additived cells were discharged after a charge-stand for a week at 25 °C. From these data (Figure 11), the self-discharge rate is found to be less than 0.5% per day. The cells were cycled at $C/5$ rate at 25 °C for over 50 cycles, and the data (Figure 12) suggest that there is little deterioration in performance. It is noteworthy that the utilization capacity values for the positive electrodes with tin oxide coated Dynel fibres are higher althrough the 50 charge–discharge cycles shown in Figure 12(a), in relation to lead–acid cells employing conventional electrodes. This also results in an enhanced utilization capacity for the lead–acid cells employing these positive electrodes in relation to the conventional lead–acid cells as shown in Figure 12(b).

The cells were discharged at different current density values ranging between 20 and 120 mA g^{-1}, and the corresponding initial drop in the cell voltage during discharge for both type of cells are shown in Figure 13(a)–(f). When a constant discharge current is applied to a freshly charged lead–acid cell, a voltage dip followed by a rise in voltage to a new plateau value, called the peak voltage, is observed at the beginning of the voltage–time curve, which is referred to as *coup de fouet* [33–35]. The voltage dip in the *coup de fouet* region is due to the supersaturated solution of bivalent lead-ions and rapid nucleation and crystallization of lead sulfate crystals on the lead dioxide surface of a charged positive plate occurring temporarily during discharge. The *coup de fouet* analysis from Figure 13, shows that the cycle life of cells with additive would be better in comparison with the conventional cells due to lower crystallization overvoltage.

4. Conclusions

2V/1.5 Ah positive limited lead–acid cells were assembled employing tin oxide coated Dynel fibres with the positive plate active material, and characterized under various operational conditions. The tin oxide coating onto Dynel fibres was made possible by a novel, rapid-thermally-activated chemical reaction process. The faradaic efficiency of the cells was found to be about 90% at $C/5$ rate at 25 °C. The discharge capacity values of the cells at $2C$ rate at 25 °C with regard to their nominal discharge capacity at $C/5$ rate are observed to be about 60%. At $C/5$ discharge rate, the cells are found to yield 110% and 45% of their nominal capacity values at 40 °C and −40 °C, respectively. The self-discharge rate for the cells was found to be $<0.5\%$ per day. The additived lead–acid cells also exhibited lower charge-transfer resistance compared to conventional cells. In brief, it has been possible to improve the positive active-mass utilization in lead–acid cells by coating Dynel-fibre additive with tin oxide, and particularly so at higher discharge rates.

References

1. K. McGregor, *J. Power Sources* **59** (1996) 31.
2. H. Dietz, J. Garche and K. Weisener, *J. Power Sources* **14** (1985) 305.
3. K.R. Bullock, *J. Electrochem. Soc.* **126** (1979) 1848.
4. W.A. Badaway and S.S. El-Egamy, *J. Power Sources* **55** (1995) 11.
5. G.L. Wei and J.-R. Wang, *J. Power Sources* **52** (1994) 25.
6. S.V. Baker, P.T. Moseley and A.D. Turner, *J. Power Sources* **27** (1989) 127.
7. H. Dietz, J. Garche and K. Weisener, *J. Appl. Electrochem.* **17** (1987) 473.
8. D.B. Edwards and V.S. Srikanth, *J. Power Sources* **34** (1991) 217.
9. A. Tokunaga, M. Tsubota and K. Yonezu, *J. Electrochem. Soc.* **136** (1989) 33.
10. B. Szczesniak, J. Kwasnik, J.D. Milewski and T. Pukacka, *J. Power Sources* **53** (1995) 119.
11. S. Wang, B. Xia, G. Yin and P. Shi, *J. Power Sources* **55** (1995) 47.
12. C.S. Ramanathan, *J. Power Sources* **35** (1991) 83.
13. L.T. Lam, O. Lim, H. Ozgun and D.A.J. Rand, *J. Power Sources* **48** (1994) 83.
14. W.-H. Kao and K.R. Bullock, *J. Electrochem. Soc.* **139** (1992) L41.
15. W.-H. Kao, S.l. Haberichter and P. Patel, *J. Electrochem. Soc.* **141** (1994) 3300.
16. K.R. Bullock, *J. Power Sources* **51** (1994) 1.
17. G.-L. Wei and J.-R. Wang, *J. Power Sources* **52** (1994) 81.
18. E. Voss, U. Hullmeine and A. Winsel, *J. Power Sources* **30** (1990) 33.
19. H. Metzendorf, *J. Power Sources* **7** (1982) 281.
20. D. Pavlov, *J. Electrochem. Soc.* **139** (1992) 3075.
21. L.T. Lam, N.P. Haigh, O.V. Lim, D.A.J. Rand and J.E. Manders, *J. Power Sources* **78** (1999) 139.
22. S. Zhong, Y.-H. Zhou and C.-S. Cha, *J. Power Sources* **70** (1998) 205.
23. N.E. Bagshaw, *J. Power Sources* **67** (1997) 105.
24. T. Rogachev and D. Pavlov, *J. Power Sources* **64** (1997) 51.
25. P.T. Moseley, *J. Power Sources* **64** (1997) 47.
26. I. Kurisawa, M. Shiomi, S. Ohsumi, M. Iwata and M. Tsubota, *J. Power Sources* **95** (2001) 125.
27. S.A. Shivashankar, A.K. Shukla, A.U. Mane, B. Hariprakash and S.A. Gaffoor, *US Patent Application* (2003).
28. B. Hariprakash, A.U. Mane, S.K. Martha, S.A. Gaffoor, S.A. Shivashankar and A.K. Shukla, *Electrochem. Solid State Lett.* **7** (2004) A66.
29. L. Liu, *Science* **199** (1978) 422.
30. JCPDS-International Centre for Diffraction Data (1997) 33–1374.
31. A.K. Shukla and B. Hariprakash, *Current Science* **85** (2003) 252.
32. B.A. Boukamp, 'Equivalent Circuit' Users Manual, University of Twente, The Netherlands (1989).
33. P.E. Pascoe and A.H. Anbuky, *INTELEC* (2000) p. 589.
34. C.S.C. Bose and C. Laman, *INTELEC* (2000) p. 597.
35. P.E. Pascoe and A.H. Anbuky, *J. Power Sources* **11** (2002) 304.